Contents lists available at ScienceDirect

EBioMedicine

Research Paper

Crohn's disease-associated *ATG16L1* T300A genotype is associated with improved survival in gastric cancer

Changqing Ma[a,*], Chad E. Storer[b], Uma Chandran[c], William A. LaFramboise[d,1], Patricia Petrosko[d,1], Madison Frank[a], Douglas J. Hartman[a], Liron Pantanowitz[a,2], Talin Haritunians[e], Richard D. Head[b], Ta-Chiang Liu[f,*]

[a] *Department of Pathology, University of Pittsburgh School of Medicine, 200 Lothrop Street, A-610, Pittsburgh, PA 15213, United States*
[b] *Department of Genetics, Washington University School of Medicine, Saint Louis, MO 63110, United States*
[c] *Department of Biomedical Informatics, University of Pittsburgh School of Medicine, Pittsburgh, PA 15213, United States*
[d] *UPMC Hillman Cancer Center, Cancer Genomics Facility, Pittsburgh, PA 15232, United States*
[e] *F. Widjaja Family Foundation Inflammatory Bowel and Immunobiology Research Institute, Cedars-Sinai Medical Center, Los Angeles, CA, United States*
[f] *Departments of Pathology and Immunology, Washington University School of Medicine, 660 South Euclid Avenue, Campus Box 8118, Saint Louis, MO 63110, United States*

ARTICLE INFO

ABSTRACT

Background: A non-synonymous single nucleotide polymorphism of the *ATG16L1* gene, T300A, is a major Crohn's disease (CD) susceptibility allele, and is known to be associated with increased apoptosis induction in the small intestinal crypt base in CD subjects and mouse models. We hypothesized that *ATG16L1* T300A genotype also correlates with increased tumor apoptosis and therefore could lead to superior clinical outcome in cancer subjects.
Methods: T300A genotyping by Taqman assay was performed for gastric carcinoma subjects who underwent resection from two academic medical centers. Transcriptomic analysis was performed by RNA-seq on formalin-fixed paraffin-embedded cancerous tissue. Tumor apoptosis and autophagy were determined by cleaved caspase-3 and p62 immunohistochemistry, respectively. The subjects' genotypes were correlated with demographics, various histopathologic features, transcriptome, and clinical outcome.
Findings: Of the 220 genotyped subjects, 163 (74%) subjects carried the T300A allele(s), including 55 (25%) homozygous and 108 (49%) heterozygous subjects. The T300A/T300A subjects had superior overall survival than the other groups. Their tumors were associated with increased CD-like lymphoid aggregates and increased tumor apoptosis without concurrent increase in tumor mitosis or defective autophagy. Transcriptomic analysis showed upregulation of WNT/β-catenin signaling and downregulation of PPAR, EGFR, and inflammatory chemokine pathways in tumors of T300A/T300A subjects.
Interpretation: Gastric carcinoma of subjects with the T300A/T300A genotype is associated with repressed EGFR and PPAR pathways, increased tumor apoptosis, and improved overall survival. Genotyping gastric cancer subjects may provide additional insight for clinical stratification.

1. Introduction

Our knowledge of cancer genetics has centered on oncogenes and tumor suppressor genes [1,2]. Recent studies have demonstrated that single nucleotide polymorphisms (SNPs) are also associated with susceptibility to sporadic cancers [3−5]. To date, genome-wide association studies (GWAS) have identified nearly a thousand predisposition variants significantly associated with over thirty malignancies [5−12]. These alterations have provided insights into new pathways for tumorigenesis and new targets for therapeutics [5]. Although most variants demonstrate a modest increase in risk [5], the combined effects of multiple SNPs are potentially useful in population-based cancer risk stratification and prevention programs [13,14]. Likewise, GWAS studies have also identified SNPs associated with response to chemotherapy [15], treatment-related toxicity [16], and clinical outcomes in cancer patients [17−19]. Therefore, identifying SNPs and other genetic alterations that correlate with clinical

Research in context

Evidence before this study

Single nucleotide polymorphisms can be associated with cancer susceptibility and/or prognosis. We previously showed that the *ATG16L1* T300A variant, a major Crohn's disease susceptibility allele, induces apoptosis (through repression of the PPAR-γ pathway) in the small intestinal crypt base in CD subjects. Notably, CD subjects with the T300A/T300A genotype have more aggressive disease course after surgical resection, whereas T300A/T300A subjects with colorectal carcinoma demonstrate superior prognosis.

Added value of this study

Our results demonstrate that the T300A/T300A genotype is associated with superior overall survival, increased tumor apoptosis and repressed EGFR and PPAR pathways in gastric cancer.

Implications of all the available evidence

Genotyping of genes and variants that are not involved in oncogenic or tumor suppressor pathways may provide insight in stratifying gastric cancer subjects.

outcome may provide novel insight into the pathobiology and management of cancer.

One area of which GWAS has provided insight into disease pathogenesis which resulted in mechanistic discoveries is immune-associated disorders [20]. Common SNPs/variants that increase the susceptibility for inflammatory bowel disease (IBD), asthma, rheumatoid arthritis, and systemic lupus erythematosus have been identified [11,20−25], and some have also been associated with increased cancer risk [26]. Lessons from these informative studies have fostered functional validations of selected SNPs. Most importantly, since these SNPs may exert effects in a wide spectrum of tissue and cell types [27], exploration of the role of these SNPs in other diseases such as malignancy may yield new hypotheses and/or insights into tumorigenesis through gene-specific, tissue-specific, or environment-specific mechanisms that merit testing.

Notably, some of the SNPs identified in immune-related disorders are also common in non-disease control subjects, suggesting that evolutionarily these SNPs may have acquired important roles in maintaining tissue homeostasis [27−29]. One such example is the *ATG16L1* Thr300Ala (T300A) SNP, the most significant susceptibility SNP in the development of Crohn's disease (CD) [30]. While originally described as a key execution member of the autophagy pathway [31], *ATG16L1* is also known to affect multiple cell death pathways, including apoptosis [32] and necroptosis [33]. We and others have shown that *Atg16l1* T300A mice showed defects in secretory cell lineages in the gut, resulting in altered immunity that affects pathogen clearance [29,34,35]. Notably, CD subjects harboring *ATG16L1* T300A have more aggressive disease course after resection [32,36,37]. Interestingly, *ATG16L1* T300A also confers protection from *Escherichia coli* infection [28], but promotes *Helicobacter pylori* infection [38]. Thus, it is likely that the effect of *ATG16L1* T300A is organ- and disease-specific.

We previously showed that CD subjects and mice with *ATG16L1* T300A possessed increased apoptosis (through repression of the PPAR-γ pathway) in the small intestinal crypt base [32]. Given the role of apoptosis as a major cell death pathway employed to target cancers [39], we hypothesized that *ATG16L1* T300A may also confer increased tumor apoptosis, which could lead to improved survival in cancer. Herein we show that in gastric cancer, the T300A genotype is associated with unique histologic features, increased cancer

apoptosis without concomitant increase in cancer proliferation or autophagy deficiency, and importantly, superior overall survival.

2. Methods

2.1. Gastric cancer cases

Gastric cancer cases resected between 2008 and 2012 were retrospectively collected by searching the surgical pathology archives of the University of Pittsburgh Medical Center (UPMC). Also included were gastric cancer cases resected between 1999 and 2013 from the Barnes-Jewish Hospital/Washington University. These cases were first described by Olsen et al. [40]. The University of Pittsburgh Medical Center and the Barnes-Jewish Hospital/Washington University are both large academic medical centers well-known in the United States. Cases from both institutions were collected in the aforementioned time frame to ensure the post-surgical follow-up period is long enough (at least 5 years) for survival analysis. For each subject / case from the UPMC, the electronic medical records were reviewed and the following demographic, clinical, and pathologic information were retrieved: gender, race, age at operation, pathologic and clinical stage, lymphovascular invasion, perineural invasion, status of surgical resection margins, pre- and post-surgery treatments if received, history of *Helicobacter pylori* infection, and survival. For cases from the Barnes-Jewish Hospital, the aforementioned demographic, clinical, and pathologic information were updated and only cases with up-to-date clinical follow-up information at the time of data collection were included in this study.

2.2. Ethics statement

This study was approved by the Institutional Review Boards of the University of Pittsburgh (STUDY20050115) and the Washington University (201301164). Informed consent from all participants was waived by the IRB committees.

2.3. Histologic evaluation

Tissue sections of the carcinoma for each case were reviewed without knowledge of the T300A genotype of each subject. Histologic subtyping for each tumor was performed using criteria of the Laurén classification system [41]. Specifically, a tumor is classified as intestinal-type if the carcinoma demonstrates intestinal differentiation with glandular / tubular structure formation. A tumor is classified as diffuse-type if the carcinoma cells demonstrate lack of cohesiveness (in other words lack of adhesion with each other) and infiltrating the gastric wall as single cells or small clusters of tumor cells. A tumor is classified as mixed-type if histologic features of both intestinal-type and diffuse-type carcinomas are observed in the same tumor.

Histologic grading of each case was performed according to criteria in the eighth edition of the American Joint Committee on Cancer recommendation on cancer staging [42]. This histologic grading system is based on the extent of glandular differentiation. In particular, a well-differentiated adenocarcinoma (G1) is defined as a tumor with greater than 95% of the tumor composed of glands. A moderately-differentiated adenocarcinoma (G2) is a tumor with 50% to 95% of the tumor composed of glands. A poorly-differentiated adenocarcinoma (G3) is a tumor with 49% or less of the tumor composed of glands. In this study, a tumor with mixed differentiation such as a mixed adenoneuroendocrine carcinoma was classified as histologic grade *X* (Gx).

The presence of a CD-like lymphoid reaction was evaluated as follows. For each case, all tumor sections were evaluated at low magnification to find one section with the most intra- and peri-tumoral lymphoid aggregates. In this tumor section, the number of intra- and peri-tumoral lymphoid aggregates were counted in 3 consecutive microscopic fields using 10× objective lens and 10× eye piece (the

use of both in combination yields a $100\times$ field of examination, which corresponds to a surface area of $3\cdot8$ mm^2 using an Olympus BX46 microscope). When on average the number of lymphoid aggregates was one or more (mean number of lymphoid aggregates per $100 \times$ field $\geq$ 1), the tumor was scored as positive for CD-like lymphoid reaction.

Mitotic activity of each tumor was evaluated by counting the number of mitotic figures in the most mitotically active area in the tumor. Briefly, for each case, all tumor sections were first evaluated at low magnification to find a "hotspot" area with the most mitotic activity. In the "hotspot" area, the number of mitotic figures was then counted in 3 consecutive high-power fields (one high-power field = $400 \times$ [$40 \times$ objective lens and $10\times$ eye piece], which correspond to a surface area of $0\cdot24$ mm^2 using an Olympus BX46 microscope). The mean number of mitotic figures in one high-power field ($400\times$) was calculated for each tumor.

2.4. Genotyping

Genomic DNA was extracted from formalin-fixed paraffin-embedded (FFPE) tissue using the QIAamp DNA FFPE tissue kit (Qiagen Inc., Valencia, CA, catalog number: 56404) and subsequently used for T300A genotyping with TaqMan® SNP Genotyping Assay (Thermo Fisher Scientific, catalog number: 4351379) following the manufacturer's instructions.

2.5. Immunohistochemistry and in-situ hybridization

For cleaved caspase-3 immunohistochemistry, unstained slides were deparaffinized, followed by antigen retrieval using Trilogy (Cell Marque, catalog number: 920P-09). The slides were quenched with 10% H$_2$O$_2$ in methanol for 10 min, before being blocked with 1% bovine serum albumin and 0.1% Trizol in phosphate buffer saline for 1 h. Thereafter, primary antibody (1:200; Cell Signaling, RRID: AB_2069869) was applied overnight. After overnight incubation, goat anti-rabbit biotinylated secondary antibody (1:200; ThermoFisher Scientific, catalog number: 31820) was applied for 45 min. Signal detection was then performed by using Vectastain Elite ABC kit (Vector, catalog number: PK-6100) and DAB (Vector, RRID: AB_2336520).

Immunohistochemistry stains with CD4 (clone SP35, Ventana, catalog number: 790-4423), CD8 (clone CD8/144B, DAKO, catalog number: M7103), CD56 (clone 123C3.D5, Ventana, RRID: AB_2335987), EGFR (clone 3C6, Ventana, RRID: AB_2335974), c-MYC (clone Y69, Ventana, catalog number: 790-4628), p62 (clone 3/P62 LCK ligand, BD Biosciences, RRID:AB_398151), MLH1 (clone M1, Ventana, catalog number: 790-4535), MSH2 (clone G219-1129, Ventana, catalog number: 760-4265), MSH6 (clone 44, Ventana, catalog number: 790-4455), and PMS2 (clone EPR3947, Cell Marque, catalog number: 288M-18) antibodies were performed on unstained 4 μm tissue sections using the Ventana XT automated stainer (Ventana Medical Systems) according to the manufacturer's recommendations. All cases were tested for Epstein $-$ Barr virus (EBV) by in-situ hybridization using pre-diluted probes targeting EBV encoded early RNA (EBER, Ventana, catalog number: 760-1209) using the Ventana XT automated stainer. All cases tested for EBER were also tested for the integrity of total RNA using RNA control probe (Leica, catalog number: RS7760) and all showed adequate total RNA preservation.

2.6. Quantitative digital image analysis of CD8-positive or CD4-positive T cell density and CD56-positive NK cell density

The CD4, CD8, and CD56 stained slides were digitized using an Aperio AT2 scanner (Leica Biosystems, Buffalo Grove, IL) at 40x magnification. The CD4 immunostained slide and CD8 stained slide for each case were manually annotated to outline the areas of invasive adenocarcinoma. Non-neoplastic gastric tissue and areas of necrosis were specifically excluded from the area of analysis. The Aperio nuclear v9 algorithm, a component of the commercially available Leica/Aperio image analysis platform, was used to count the CD4- or CD8-stained cells as previously described [43]. The CD4-positive or CD8-positive T cell density was determined by dividing the number of CD4-positive or CD8-positive cells by the area (measured in mm^2) examined. Densities (number of cells / mm^2) of CD56-positive, CD4-positive, or CD8-positive cells in peri- and intratumoral lymphoid aggregates were additionally determined using the same algorithm.

2.7. Transcriptomic analysis

For each tumor included in transcriptomic analysis, a representative FFPE tumor tissue block was selected. The tumor area desired for transcriptomic analysis was manually circled on the hematoxylin and eosin stained tissue section. Manual microdissection of the desired tumor area was then performed on 6 to 10 unstained tumor tissue sections at 10 μm thickness for each tumor to ensure that only area of viable tumor but not necrosis or uninvolved tissue was included in transcriptomic analysis (Supplementary Fig. 1). Total RNA was extracted from manually dissected tumor tissue using the Qiagen miR-Neasy mini kit (Qiagen Inc., catalog number: 74104) according to the manufacturer's recommendations. RNA library was prepared using the TruSeq RNA ACCESS library preparation kit (Illumina, San Diego, CA, catalog number: 15049525). Transcriptomic analysis was performed on the NextSeq 500 system according to the manufacturer's recommendations (please see Supplementary Method for details).

Quality of the RNAseq results of all 47 cases were assessed using FastQC (v0.11.5). All 47 cases fulfilled the quality control parameters. Samples were then aligned to the GRCh38 genome with HISAT2 (v2.1.0) [44] and to the human transcriptome with Salmon (0.11.0) [45]. Alignments were quality assessed with QoRTs (v1.1.8) [46] and RNASeQC (v1.1.8) [47]. Gene expression was quantified with HTSeq (v0.9.0) [48]. Data normalization with the weighted trimmed mean of M-values (TMM) method and differential gene expression between T300A genotypes were performed with the edgeR R package [49]. Benjamini$-$Hochberg method was used for correction of multiple testing for differential gene expression.

Differentially expressed genes with $P < 0\cdot01$ were further analyzed by a novel knowledge engine called 'COmprehensive Multi-omics Platform for Biological InterpretatiOn' (CompBio: https://www.percayai.com/CompBio) [50]. CompBio performs a literature analysis to identify relevant biological processes and pathways represented by the differentially expressed entities (genes, proteins, miRNA's, or metabolites). This is accomplished with an automated Biological Knowledge Generation Engine that extracts all abstracts from PubMed that reference entities of interest (or their synonyms), using contextual language processing and a biological language dictionary that is not restricted to fixed pathway and ontology knowledge bases. Conditional probability analysis calculates the statistical enrichment of biological concepts (processes/pathways) over those that occur by random sampling. Related concepts built from the list of differentially expressed entities are further clustered into higher-level themes (e.g., biological pathways/processes, cell types and structures, etc.). The dataset was then cross-referenced with the T300A/T300A-specific transcriptomic themes identified in mouse ileum (ArrayExpress database E-MTAB-5707) [32].

2.8. Statistics

Statistical analysis was performed with GraphPad Prism 7 for Windows Version 7.00 (GraphPad Software, La Jolla, CA) and IBM SPSS (Release 23.0.0.0). GraphPad Prism 7 was used to perform both paired and unpaired Student t-tests, Mann$-$Whitney test, and Kruskal$-$Wallis test, which were used for comparison of continuous variables. IBM SPSS was used to perform survival analysis, Two-sided

Fisher's exact test, and Chi-Square test. The latter two tests were used for the comparison of categorical data. Hardy−Weinberg equilibrium testing was performed by comparing observed genotype frequencies with those expected in Caucasian subjects and in African American subjects by Chi-Square test in *R* using the package named Hardy−Weinberg (https://cran.r-project.org/web/packages/HardyWeinberg/HardyWeinberg.pdf). All tests were two-tailed and a *P* value less than $0·05$ ($P < 0·05$) was considered significant. For survival analysis, overall survival was defined as the duration between surgical resection and either death or the latest clinical follow-up time. Death occurring within one month of the initial operation was attributed to operative mortality and was not included in the survival analysis. Subjects who were clinical stage IV at the time of surgery, i.e., with distant metastasis at the time of surgery, were considered never disease free and hence excluded from the analysis for disease-free survival. Survival analysis was performed using Cox proportional hazard model and Kaplan-−Meier analysis with log-rank statistics. Potential confounding factors in univariate and/or multivariate analysis included race, histologic grade, histologic subtype by Laurén classification, clinical stage, surgical resection margin, lymphovascular invasion, perineural invasion, *Helicobacter pylori* infection, and chemotherapy.

Sequencing files are deposited at Gene Expression Omnibus (GEO) under accession number GSE152415.

2.9. Role of funding source

The funder (NIH) did not have any role in study design, data collection, data analyses, interpretation, or writing of report.

3. Results

3.1. Characteristics of the gastric cancer cohort

We retrospectively collected tissue from 220 consecutively resected gastric cancer subjects from two academic medical centers for genotyping and histopathology analysis. Among them, 163 (74%) subjects carried the T300A allele(s), including 55 (25%) homozygous T300A/T300A and 108 (49%) heterozygous T300A/wild-type (WT) subjects. Homozygous WT/WT genotype was detected in 57 (26%) subjects. The flow diagram of the gastric cancer cases analyzed in this study is shown in Fig. 1, and the demographics and clinicopathologic characteristics of the 220 genotyped subjects are listed in Table 1.

The T300A allele frequency was $0·56$ and the WT allele frequency was $0·44$ in Caucasian subjects in our cohort. In African American subjects the allele frequency was $0·23$ for the T300A allele and $0·77$

Fig. 1. *Flow chart illustrating type of analysis and number of cases.* Flow diagram of the number of subjects genotyped and the number of cases analyzed for histopathologic features, clinical outcome, and transcriptomes.

for the WT allele. Allele frequencies of the T300A SNP in our cohorts were comparable to those reported in public databases [30]. In addition, genotype frequencies in Caucasian subjects and African American subjects did not deviate from Hardy−Weinberg equilibrium ($P > 0·05$ [Chi-Square test]). Since the T300A allele is more frequent in Caucasians than in African American subjects, homozygous T300A/T300A genotype was more frequently identified in Caucasians than other genotypes ($P < 0·01$ [Fisher's exact test]; Table 1). Only 33 (15%) subjects had either clinical history or active/concurrent *Helicobacter pylori* infection. When stratified by genotype, *Helicobacter pylori* infection was more often seen in homozygous WT/WT subjects than in subjects with other genotypes (14/57, 25% versus 11/108, 10% versus 8/55, 15%). However, this difference was not statistically significant ($P = 0·07$ [Fisher's exact test]; Table 1). There was also no significant difference in the histologic degree of tumor differentiation, histologic type by the Laurén classification [41], clinical stage, receipt of pre- and post- surgical treatment, or other histopathologic parameters between different genotype groups ($P > 0·05$ for all [Fisher's exact test]; Table 1).

3.2. Gastric cancer subjects with ATG16L1 T300A/T300A showed superior prognosis after surgery

We next assessed if the *ATG16L1* T300A genotype correlated with clinical outcome. Among all 220 subjects with confirmed genotypes, those with the T300A/T300A genotype showed superior overall survival compared to the other two groups combined (WT/T300A and WT/WT) by Kaplan-−Meier survival analysis with log-rank statistics (mean, standard error, and 95% confidence interval [CI] of overall survival: 107 months, 14 months, [80−135] versus 64 months, 9 months, [52−76], $P = 0·035$) (Fig. 2a). Using Cox proportional hazards modeling, however, the T300A/T300A genotype was not an independent predictor of overall survival for the entire cohort in multivariate analysis (multivariate analysis hazard ratio and 95% CI: $0·77, 0·47 − 1·26, P = 0·31$) (Supplementary Table 1).

In order to exclude potential confounding effects on overall survival introduced by pre- and post-surgical chemotherapy, we next performed survival analysis in the subset of 126 subjects who received only surgical treatment. Among them, subjects with T300A/T300A genotype had significantly longer overall survival than subjects with WT/T300A and WT/WT genotypes combined using Kaplan-−Meier survival analysis with log-rank statistics (mean, standard error, and 95% CI: 164 months, 16 months, [132−196] versus 60 months, 5 months, [51−69], $P = 0·019$) (Fig. 2b). Using Cox proportional hazards modeling, the T300A/T300A genotype was associated with a significant increase in overall survival by both univariate and multivariate analysis (multivariate analysis hazard ratio and 95% CI: $0·31, 0·11−0·88, P = 0·03$) (Table 2).

Approximately one-third (45, 36%) of the 126 subjects with surgery as the only treatment died during the follow-up period. WT/WT subjects had significantly higher mortality than subjects with other T300A genotypes (WT/WT: 19/35, 54% versus WT/T300A: 20/57, 35% versus T300A/T300A: 6/30, 20%, $P = 0·02$ [Fisher's exact test]). The percentages of patients who died of disease progression were similar between the three groups: 7/19 (37%) in WT/WT, 7/20 (35%) in WT/T300A, and 2/6 (33%) in T300A/T300A groups ($P = 0·73$ [Fisher's exact test]). Likewise, other comorbidities and surgical complications accounted for death in 12/19 (63%) WT/WT, 13/20 (65%) in WT/T300A, and 4/6 (67%) in T300A/T300A groups (Supplementary Table 2).

3.3. T300A/T300A genotype was associated with unique histological features

We and others have previously found that T300A/T300A genotype was associated with histomorphologic changes in CD subjects and mouse models [34,51,52], including increased apoptosis induction in
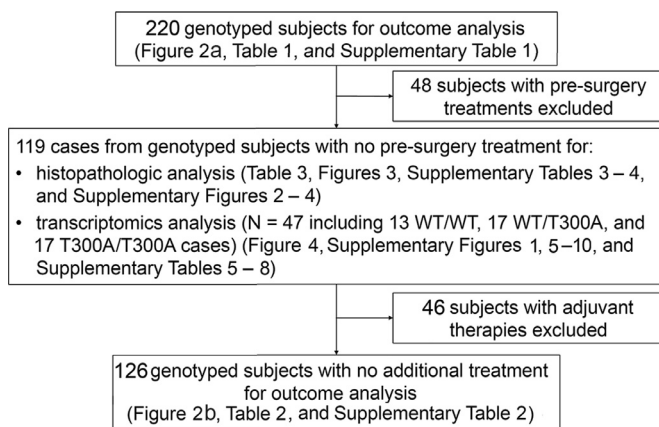
Table 1
Demographics and clinicopathologic characteristics stratified by T300A genotype.

	All cases($N = 220$)	WT/WT($N = 57$)	WT/T300A($N = 108$)	T300A/T300A($N = 55$)	P
Age (year; median, [IQR])	73 (19)	75 (15)	71 (20)	72 (22)	0.40
Gender (n, %)					
Female	96 (44)	28 (49)	48 (44)	20 (36)	0.38
Male	124 (56)	29 (51)	60 (56)	35 (64)	
Race (n, %)	$N = 167$	$N = 41$	$N = 82$	$N = 44$	
Caucasian	135 (81)	24 (59)	71 (87)	40 (91)	< 0.01
African American	20 (12)	13 (32)	5 (6)	2 (5)	
Others	12 (7)	4 (10)	6 (7)	2 (5)	
Histologic type (n, %)					
Intestinal	104 (47)	31 (54)	45 (42)	28 (51)	0.48
Diffuse	84 (40)	18 (32)	49 (45)	20 (36)	
Mixed and other types	29 (13)	8 (14)	14 (13)	7 (13)	
Histologic grade (n, %)					
G1	14 (6)	2 (4)	7 (6)	5 (9)	0.14
G2	57 (26)	21 (37)	20 (19)	16 (29)	
G3	146 (66)	33 (58)	79 (73)	34 (62)	
Gx	3 (1)	1 (2)	2 (2)	0	
Clinical stage (n, %)					
I	72 (33)	17 (30)	31 (29)	24 (44)	0.10
II	58 (26)	20 (35)	25 (23)	13 (24)	
III	62 (28)	16 (28)	32 (30)	14 (25)	
IV	26 (12)	3 (5)	19 (18)	4 (7)	
Unknown	2 (1)	1 (2)	1 (1)	0	
Positive resection margin (n, %)	34 (15)	8 (14)	20 (19)	6 (11)	0.44
Positive lymphovascular invasion (n, %)	135 (61)	33 (58)	71 (66)	31 (56)	0.31
Positive perineural invasion (n, %)	93 (42)	21 (37)	52 (48)	20 (36)	0.29
Helicobacter pylori infection (n, %)	33 (15)	14 (25)	11 (10)	8 (15)	0.07
Vital status (at the time of data collection) (n, %)					
Alive	93 (43)	21 (37)	43 (40)	29 (53)	0.24
Death	121 (55)	34 (60)	61 (56)	26 (47)	
Lost to follow-up	6 (3)	2 (4)	4 (4)	0	
Overall follow-up time (month; median, [IQR])	25 (46)	21 (51)	20 (41)	37 (53)	0.02
Recurrence (at the time of data collection) (n, %)	$N = 178$	$N = 49$	$N = 81$	$N = 48$	
No	116 (65)	30 (61)	56 (69)	31 (65)	0.73
Yes	62 (35)	19 (39)	26 (32)	17 (35)	
Disease free time (month; median, [IQR])	23 (46)	18 (45)	22 (48)	25 (44)	0.37
Chemotherapy (n, %)					
None	126 (57)	36 (63)	60 (56)	30 (55)	0.79
Neoadjuvant only	13 (6)	2 (4)	7 (6)	4 (7)	
Adjuvant only	46 (21)	13 (23)	23 (21)	10 (18)	
Both	35 (16)	6 (11)	18 (17)	11 (20)	

Abbreviations: WT: wild-type; IQR: interquartile range; G: grade.
Kruskal-—Wallis test was used for comparison of continuous variables. Fisher's Exact Test was used for the comparison of categorical data.

small intestinal crypt base where Paneth cells and intestinal stem cells (both are CD-relevant cell types) reside [53]. We therefore hypothesized that T300A/T300A genotype was also associated with unique histologic features in gastric cancer. To exclude the possibility that neoadjuvant therapy may affect histologic features, we performed histologic assessments of the tumors from subjects who did not receive neoadjuvant therapies, including subjects who received no additional treatment either before or after surgery and those who received only adjuvant treatment. Cases with tumor blocks available (n = 119) were included in histologic evaluation (Fig. 1). As shown in Supplementary Table 3, there was no significant difference in *Helicobacter pylori* infection, the histologic degree of tumor differentiation, histologic subtype, clinical stage, or other histologic features between different genotype groups ($P > 0 \cdot 05$ for all [Fisher's exact test]).

In contrast, we found that the T300A/T300A tumors were more likely to contain intra- and peri-tumoral CD-like lymphoid aggregates than homozygous WT/WT tumors (25/28, 89% versus 21/32, 66%, $P = 0 \cdot 037$ [Fisher's exact test]) (Fig. 3a, b, and Table 3). We further analyzed the density of lymphocytes not associated with lymphoid aggregates, using an unbiased automated image analysis system [43]. There was no difference in the density of CD8-positive or CD4-positive *T* cells at the tumor invasive front (tumor-stroma interface) ($P = 0 \cdot 60$ and 0.89, respectively, [Kruskal-—Wallis test]) or within the tumors ($P = 0 \cdot 72$ and 0.61, respectively, [Kruskal-—Wallis test]) (Supplementary Table 4 and Supplementary Fig. 2). We additionally

analyzed the density of CD4-positive *T* cells, CD8-positive *T* cells, and CD56-positive NK cells in peri- and intratumoral lymphoid aggregates using the same automatic image analysis system [43]. These lymphoid aggregates contained similar proportions of CD4-positive *T* cells and CD8-positive *T* cells (mean and standard deviation: CD4-positive *T* cell density: 1587 ± 618 versus CD8-positive *T* cell density: 1556 ± 611; $P = 0 \cdot 78$ [paired *t*-test]). The ratio of CD4-positive cell density and CD8-positive cell density was not associated with tumor T300A genotypes (mean and standard deviation of CD4 cell density / CD8 cell density: WT/WT: $1 \cdot 06 \pm 0 \cdot 38$ versus T300A/T300A: $1 \cdot 11 \pm 0 \cdot 76$; $P = 0 \cdot 63$ [Mann-—Whitney test]) (Supplementray Figs. 3a, c, and d). In contrast CD56-positive NK cell was not a significant component in peri- and intratumoral lymphoid aggregates (Supplementray Figs. 3b and e).

3.4. T300A/T300A genotype was associated with increased tumor apoptosis

Given the role of *ATG16L1* T300A in mediating various cell death pathways, predominantly autophagy and apoptosis, we next determined if proliferation, autophagy, and apoptosis were differentially correlated with subject genotypes. We found that there was no difference in the mitotic activities in the tumors of the T300A/T300A group compared to the others ($P = 0 \cdot 64$ [Kruskal-—Wallis test]) (Supplementary Figs. 4a, b, and Supplementary Table 4). Likewise, as a
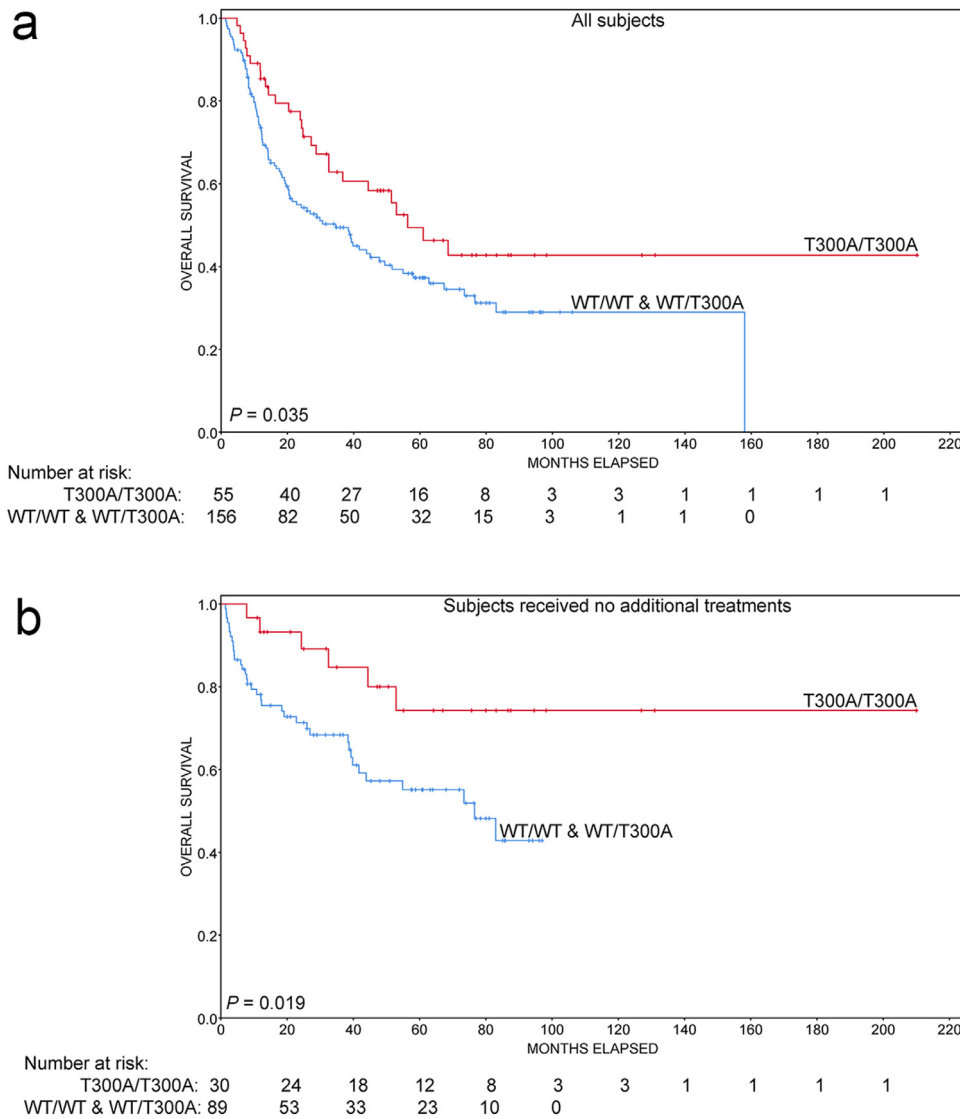
Fig. 2. *Gastric cancer subjects with T300A/T300A genotype had superior overall survival.* Kaplan-–Meier survival analysis using log-rank statistics comparing the overall survival of subjects with gastric carcinoma stratified by T300A genotype in the entire cohort ($n = 220$, $P = 0\cdot035$ [log-rank]) (a) and in the subset of subjects without additional pre- or post-surgical treatment ($n = 126$, $P = 0\cdot019$ [log-rank]) (b).

Table 2

Univariate and multivariate analysis of overall survival in subjects without additional treatment ($N = 126$) by Cox regression.

No additional treatment cases ($N = 126$)	Univariate analysis			Multivariate analysis		
	P	HR	95% CI	P	HR	95% CI
T300A/T300A	0.02	0.37	0.16−0.88	0.03	0.31	0.11−0.88
African American	0.31	0.61	0.24−1.58			
High histologic grade	0.71	0.89	0.49−1.64			
Diffuse type histology	0.59	0.82	0.40−1.68			
Stage III & IV	< 0.001	6.0	2.98−12.24	0.02	3.0	1.16−7.74
Positive surgical resection margin	0.01	2.85	1.24−6.56	0.96	0.97	0.32−2.94
Lymphovascular invasion	< 0.001	5.45	2.57−11.57	< 0.001	4.11	1.86−9.07
Perineural invasion	0.04	1.96	1.04−3.72	0.71	1.17	0.52−2.61
Helicobacter pylori infection	0.51	0.74	0.31−1.78			

Abbreviations: HR: hazard ratio; CI: confidence interval.

readout for autophagy activation, the prevalence of p62-positive immunohistochemical staining was similar between all groups ($P = 0\cdot27$ [Chi-Square test]) (Supplementary Figs 4c, d, and Supplementary Table 4). In contrast, the T300A/T300A tumors showed significantly increased intratumoral apoptosis compared with tumors of other genotypes ($P = 0\cdot04$ [Kruskal-–Wallis test]) by cleaved-caspase 3 immunohistochemistry (Figs. 3c, d, e, f, and Table 3). Therefore, the T300A/T300A genotype was associated with increased intratumoral apoptosis without concurrent changes in autophagy activation or mitosis.

3.5. Gastric cancer from T300A/T300A subjects showed unique transcriptomic signatures

To further characterize the pathways that may be involved in mediating the apoptosis induction in the T300A/T300A tumors, we performed global transcriptomics on a subset of 47 tumors that did not receive neoadjuvant therapies (including 13 WT/WT, 17 WT/T300A, and 17 T300A/T300A cases) (Fig. 1). Of note, since gastric carcinoma with DNA mismatch repair (MMR) protein deficiency
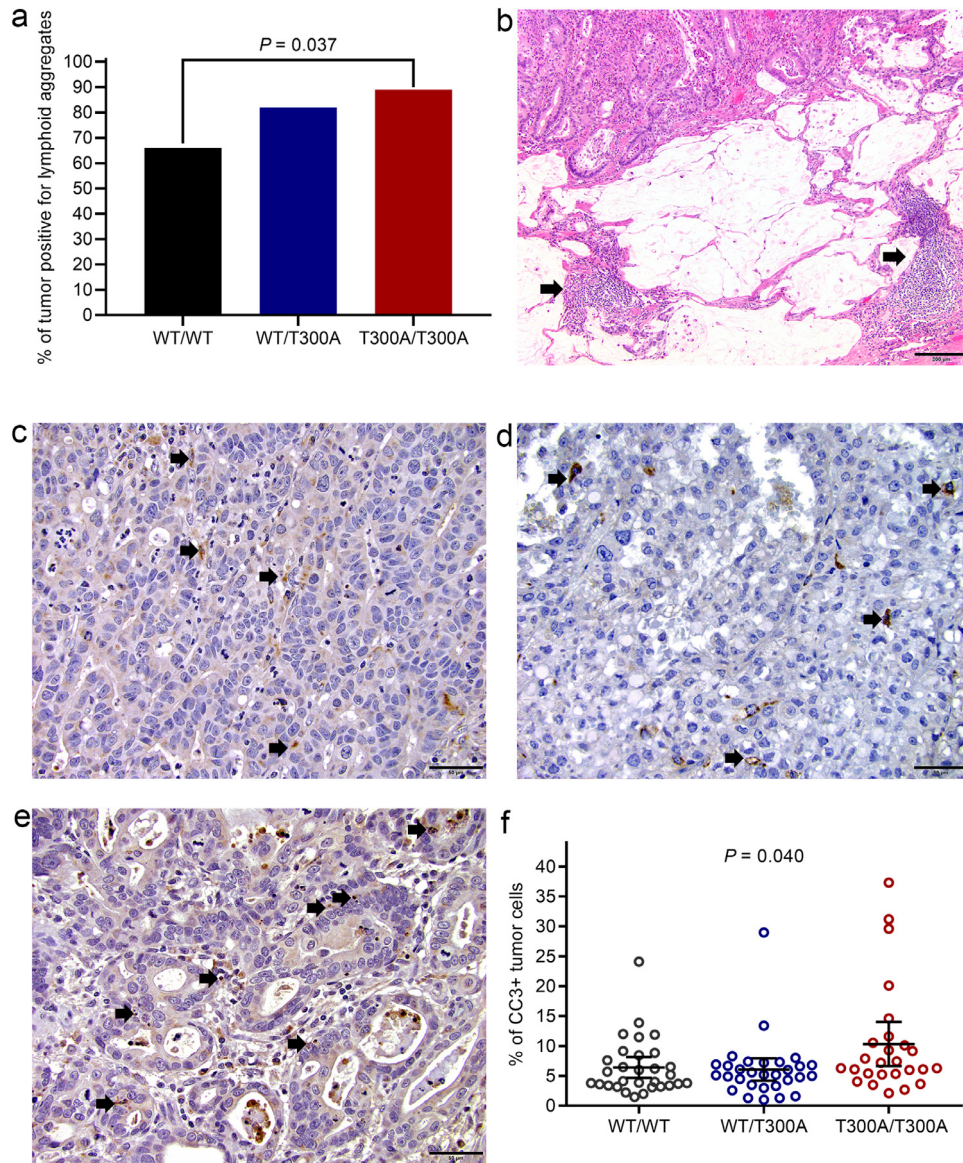
Fig. 3. *Tumors from T300A/T300A subjects showed more lymphoid aggregates and apoptosis.* (a) T300A/T300A tumors were more likely to have intra- and peritumoral lymphoid aggregates than WT/WT tumors (*P* = 0·037 [Fisher's exact test]) (WT/WT *n* = 32, WT/T300A *n* = 55, T300A/T300A *n* = 28). (b) Representative photomicrograph of a gastric adenocarcinoma with intra- and peritumoral lymphoid aggregates (arrows). (c) Representative photomicrograph of a WT/WT tumor with 6% of cleaved-caspase 3-positive (CC3+) tumor cells (arrows) / 400× field on average in 5 representative fields. (d) Representative photomicrograph of a WT/T300A tumor with 6% of CC3+ tumor cells (arrows) / 400× field on average in 5 representative fields. (e) Representative photomicrograph of a T300A/T300A tumor with 10% of CC3+ tumor cells (arrows) / 400× field on average in 5 representative fields. (f) T300A/T300A tumors had significantly increased CC3+ tumor cells compared with tumors of the other two genotypes (*P* = 0·04 by ANOVA) (WT/WT *n* = 30, WT/T300A *n* = 30, T300A/T300A *n* = 26). Error bars represent mean with 95% confidence interval. Scale bars: b-200 μm; c, d, e-50 μm.

Table 3

Tumor immune microenviroment and apoptosis by cleaved-caspase3 immunoistochemistry stratified by T300A genotype.

	WT/WT	WT/T300A	T300A/T300A	P^1	P^2	P^3
Peri- and intra-tumoral lymphoid aggregates (*n*, %)	*N* = 32	*N* = 55	*N* = 28			
Negative (< 1 / 100 × field)	11 (34)	10 (18)	3 (11)	0.06	0.18	0.037
Positive (≥ 1 / 100 × field)	21 (66)	45 (82)	25 (89)			
No. of cases stained for CC3	*N* = 30	*N* = 30	*N* = 26			
% of CC3-positive tumor cells / 400× field (median, [IQR])	4.7 (5.1)	5.2 (3.5)	6.8 (5.5)	0.04	0.01	0.04

Kruskal-–Wallis test and Mann-–Whitney test were used for comparison of continuous variables. Fisher's exact test was used for the comparison of categorical data.

Abbreviations: WT: wild-type; IQR: interquartile range; CC3: cleaved-caspase 3.

[1] *P*-value for the comparison between all three groups.

[2] *P*-value for the comparison between WT/WT and WT/T300A combined and T300A/T300A (WT/WT & WT/T300A vs. T300A/T300A).

[3] *P*-value for the comparison between WT/WT and T300A/T300A.

/microsatellite instability (MSI) or Epstein - Barr virus (EBV) infection have distinct molecular features [54], tumors that were MMR deficient/MSI or EBV-positive were also excluded from transcriptomic analysis. Manual microdissection was also performed to ensure that only area of viable tumor and not necrosis or uninvolved tissue was submitted for bulk transcriptomic analysis for each tumor to minimize potential transcriptomic variations caused by differences in cell types (Supplementary Fig. 1). Transcriptomic analysis yielded 487 significantly expressed genes associated with the T300A/T300A genotype, including 296 upregulated genes and 191 downregulated genes ($P < 0.001$) (Fig. 4a and Supplementary Table 5). These were used subsequently in pathway analysis.

Using a novel biological knowledge generation engine (CompBio) [50], we identified biological processes that were associated with

Fig. 4. *Transcriptomic analysis identified gene signatures associated with T300A/T300A genotype in gastric cancer.* (a) Intensity plot of normalized gene expression level for 487 significantly expressed genes ($P < 0.01$) associated with the T300A/T300A genotype (WT/WT & WT/T300A n = 30, T300A/T300A n = 17). (b) Transcriptomic themes from genes upregulated in the T300A/T300A tumors performed by CompBio analysis. (c) Themes from genes downregulated in the T300A/T300A tumors performed by CompBio analysis.

cancers from subjects with different genotypes. The T300A/T300A tumors showed upregulation of genes involved in the following themes: embryonic stem cell reprogramming, immunoglobulin, WNT/β-catenin signaling, and microvessel density (Fig. 4b and Supplementary Fig. 5). In addition, these tumors also showed repression of expression of genes involved in the following transcriptomic themes: PPAR pathway, EGFR signaling, and inflammatory chemokines (*CCL2, CXCL2, CCL13, CCL3l3, IL-6*), among others (Fig. 4c and Supplementary Fig. 6). Previous studies demonstrated that the T300A mutation is associated with type I interferon (IFN) activation in colon cancer cells *in vitro* [55] and in mouse model [29]. A type I IFN mRNA expression signature was not detected in T300A/T300A tumors in our cohort (Supplementary Fig. 7 and Supplementary Table 6).

Immunohistochemistry study of selected genes with up regulated (*c-MYC*) and down regulated (*EGFR*) RNA expression in T300A/T300A tumors demonstrated strong c-MYC staining but a lack of EGFR staining in T300A/T300A tumors (Supplementary Figs. 8 and 9). In contrast, WT/WT or WT/T300A tumors showed strong EGFR staining without c-MYC staining. These findings support that gene expression alterations observed from transcriptomic analysis are associated with tumor T300A genotypes.

Finally, to understand how much the transcriptomic themes identified are generalizable between different tissue types, we also compared the data to our previously published dataset where full-thickness ileal tissue between T300A/T300A and WT/WT mice were compared [32]. Using CompBio, we identified several common transcriptomic themes between the two datasets. Most of the transcriptomic themes identified as upregulated in the T300A/T300A gastric cancers were also seen in the T300A/T300A mouse ileum (Supplementary Fig. 10a) whereas themes associated with mesenchymal stem cells, retinoic acid signaling, chemokines, and PPAR signaling were common downregulated transcriptomic themes between the T300A/T300A gastric cancers and T300A/T300A mouse ileum (Supplementary Fig. 10b). Overlapping genes in association with the T300A/T300A between the two datasets are shown in Supplementary Tables 7 and 8. Therefore, despite the species and organ differences, we identified common transcriptomic themes associated with the T300A/T300A genotype.

4. Discussion

Recent advances in cancer genetics have focused on genes whose functions are beyond the roles of oncogenes and tumor suppressor genes. In particular, genetic studies from immune-associated diseases have shown that common SNPs can be associated with disease-relevant pathophysiologic changes. In the current study, we hypothesized that a well-studied SNP associated with CD susceptibility, *ATG16L1* T300A, may be associated with survival difference in cancer subjects. We showed that the T300A/T300A genotype was associated with superior overall survival in gastric cancer subjects. Histologically, the T300A/T300A genotype was associated with CD-like lymphoid aggregates and prominent cancer cell apoptosis. Finally, the molecular signatures associated with these tumors provided possible mechanisms by which the T300A allele functions.

In contrast to its survival benefit in gastric cancer demonstrated in our study, the T300A/T300A genotype is associated with more aggressive clinical phenotype and disease course in CD [32,56]. The dichotomy may be due to the biologic processes involved in different disease contexts. In CD, increased crypt base apoptosis leads to Paneth cell defect, resulting in diminished innate immunity and dysbiosis, whereas, in gastric cancer, increased tumor apoptosis without concomitant increase in tumor proliferation leads to improved survival. This is supported by a recent study demonstrating the T300A phenotype differences are stimulation (environmental factors)- and cell type-dependent [57]. On the other hand, survival benefit of the T300A/T300A genotype has also been shown in colorectal and non-
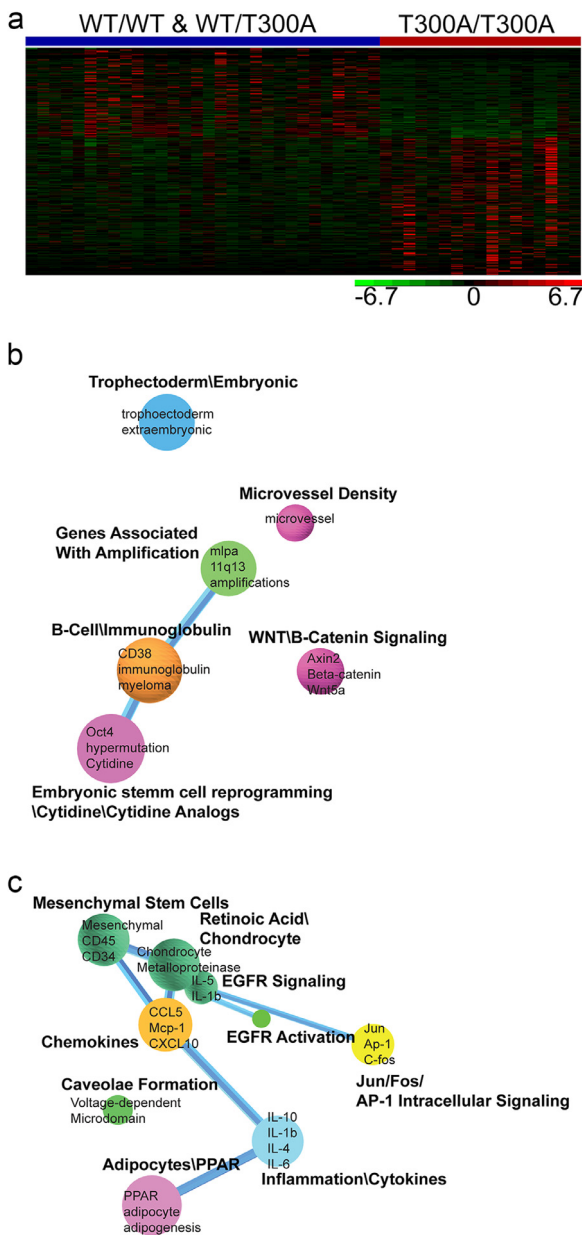
small cell lung cancers [55,58]. Our study suggests that the protective effect of the T300A may be common to multiple cancer types, although the mechanisms by which T300A confers improved survival may be organ-specific. In particular, the T300A/T300A genotype was not associated with a decrease in clinical stage IV/metastatic gastric carcinoma in our cohort. More importantly, the main molecular pathways associated with T300A in gastric carcinoma may be different from pathways identified in colon cancer. Type I IFN activation was detected in human colon cancer cell line with T300A mutation [55] but was not detected in gastric carcinoma with T300A/T300A genotype.

Notably, the *ATG16L1* T300A variant has been associated with susceptibility of gastric cancer. In the study by Burada et al., the risk of developing gastric carcinoma was significantly reduced (odds ratio: $0 \cdot 52$, 95% confidence interval $0 \cdot 13 - 0 \cdot 88$, $P = 0 \cdot 013$) in subjects carrying the T300A allele compared with those with WT/WT genotype in a cohort of 350 Romanian subjects [59]. In contrast, the T300A allele was associated with an increased risk of gastric carcinoma (adjusted odds ratio: $2 \cdot 38$, 95% confidence interval $1 \cdot 34 - 4 \cdot 24$, $P = 0 \cdot 003$) in 304 ethnic Chinese subjects [60]. These findings suggest that the *ATG16L1* T300A allele may be associated with susceptibility of gastric cancer but its impact may be population specific. Additionally, studies performed in Crohn's disease have shown that the genetics underlying disease prognosis may be independent of the genetics underlying disease susceptibility [61]. Further validation of the association between T300A genotype and gastric cancer susceptibility will ideally require studying large numbers of subjects, as has been performed in other disease types [3−5,30,61−64]. However, our findings together with results in colon and non-small cell lung cancers may imply a survival benefit of the T300A allele against carcinoma. In addition, we feel, this protective effect may be generalizable to wider populations given the relatively large number of subjects from different geographic areas included in our study (St. Louis and Pittsburgh, U.S.) and studies of colorectal carcinoma ($n = 460$, Chicago, U.S.) [55] and non-small cell lung cancer ($n = 323$, China) [58].

A unique feature of our study is the focus on transcriptomics of tumors that are not associated with known outcome confounders such as MSI or EBV infection, as these are also known to have distinct pathogenic pathways [54,65,66]. In addition, we have also focused our analysis on subjects who did not receive pre-surgery treatment, such that the histopathologic and transcriptomic readouts were not affected by other therapeutic modalities.

Our transcriptomic study provides insight into the etiopathogenesis by which SNP variants of autophagy genes may modulate tumor biology. Importantly, despite the difference in species and organs, we were able to validate key transcriptomic themes in the gastric cancer dataset specific to T300A/T300A genotype using our previously published mouse model [32]. The correlation between the T300A/T300A genotype and repressed PPAR signaling is also in keeping with our previous study in CD patients and mouse model which showed that hosts with T300A were prone to have repressed PPAR-γ signaling [32]. It further validates our previous mouse model by which repressed PPAR signaling directly links to increased apoptosis [32]. Our data is also consistent with a previous study which showed that activated PPAR signaling negatively correlated with prognosis in gastric cancer patients, possibly through regulating lipid and fatty acid metabolism [67]. Therefore, one possible mechanism by which T300A confers survival benefit in gastric cancer is through repression of PPAR pathway. As PPAR agonists are being developed for gastric cancer patients [67,68], our study provides a unique insight into the patient population that may benefit most from this therapy.

Potential limitations of our study include the retrospective study design, and the lack of *in vitro* and/or *in vivo* studies to further define the role of the identified molecular pathways. Prospective studies with a larger cohort with more complete clinical data and *in vitro/in*

vivo studies for mechanisms are needed to validate the findings described in our study.

In summary, we showed that CD susceptibility allele *ATG16L1* T300A was associated with improved survival in gastric cancer subjects, in contrast to its prognostic implication in CD. As the T300A genotype is also prevalent in non-IBD subjects [30], our data suggests a possible evolutionary benefit in the setting of non-IBD. Furthermore, genotyping of genes that are not involved in oncogenic or tumor suppressor pathways may provide insight in stratifying subjects.

Contributors

CM and TCL designed the study. CM, WAL, PP, MF, DJH, and LP acquired data. CM, CS, UC, RH, TH, and TCL analyzed data. CM and TCL verified the data. CM and TCL drafted the manuscript.

All authors reviewed and approved the manuscript.

Data sharing statement

The RNA-seq data generated in this manuscript are available at NCBI's Gene Expression Omnibus and publicly accessible through GEO Series accession number GSE152415 (https://www.ncbi.nlm.nih.gov/geo/query/acc.cgi?acc=GSE152415).

Declaration of Competing Interest

R.D. Head and C. E. Storer may receive royalty income based on the CompBio technology developed by R.D. Head and licensed by Washington University to PercayAI.

L. Pantanowitz is a member of the medical advisory board for Ibex and reports personal fees from Ibex.

D.J. Hartman reports personal fees from Genae (adjudication work) and Up-To-Date (royalty for educational content).

The other authors have declared that no conflict of interest exists.

Acknowledgments

Supplementary materials

Supplementary material associated with this article can be found in the online version at doi:10.1016/j.ebiom.2021.103347.

References

[1] Tomasetti C, Marchionni L, Nowak MA, Parmigiani G, Vogelstein B. Only three driver gene mutations are required for the development of lung and colorectal cancers. Proc Natl Acad Sci USA 2015;112:118–23.

[2] Bailey MH, Tokheim C, Porta-Pardo E, Sengupta S, Bertrand D, Weerasinghe A, et al. Comprehensive characterization of cancer driver genes and mutations. Cell 2018;173:371–85 e18.

[3] Lichtenstein P, Holm NV, Verkasalo PK, Iliadou A, Kaprio J, Koskenvuo M, et al. Environmental and heritable factors in the causation of cancer–analyses of cohorts of twins from Sweden, Denmark, and Finland. N Engl J Med 2000;343:78–85.

[4] Fletcher O, Houlston RS. Architecture of inherited susceptibility to common cancer. Nat Rev Cancer 2010;10:353–61.

[5] Sud A, Kinnersley B, Houlston RS. Genome-wide association studies of cancer: current insights and future perspectives. Nat Rev Cancer 2017;17:692–704.

[6] Abnet CC, Freedman ND, Hu N, Wang Z, Yu K, Shu XO, et al. A shared susceptibility locus in PLCE1 at 10q23 for gastric adenocarcinoma and esophageal squamous cell carcinoma. Nat Genet 2010;42:764–8.

[7] Helgason H, Rafnar T, Olafsdottir HS, Jonasson JG, Sigurdsson A, Stacey SN, et al. Loss-of-function variants in ATM confer risk of gastric cancer. Nat Genet 2015;47:906–10.

[8] Shi Y, Hu Z, Wu C, Dai J, Li H, Dong J, et al. A genome-wide association study identifies new susceptibility loci for non-cardia gastric cancer at 3q13.31 and 5p13.1. Nat Genet 2011;43:1215–8.

[9] Mocellin S, Verdi D, Pooley KA, Nitti D. Genetic variation and gastric cancer risk: a field synopsis and meta-analysis. Gut 2015;64:1209–19.

[10] Milne RL, Kuchenbaecker KB, Michailidou K, Beesley J, Kar S, Lindström S, et al. Identification of ten variants associated with risk of estrogen-receptor-negative breast cancer. Nat Genet 2017;49:1767–78.

[11] Noguchi E, Sakamoto H, Hirota T, Ochiai K, Imoto Y, Sakashita M, et al. Genome-wide association study identifies HLA-DP as a susceptibility gene for pediatric asthma in Asian populations. PLoS Genet 2011;7:e1002170.

[12] Huang KL, Mashl RJ, Wu Y, Ritter DI, Wang J, Oh C, et al. Pathogenic germline variants in 10,389 adult cancers. Cell 2018;173:355–70.

[13] Lecarpentier J, Silvestri V, Kuchenbaecker KB, Barrowdale D, Dennis J, McGuffog L, et al. Prediction of breast and prostate cancer risks in male BRCA1 and BRCA2 mutation carriers using polygenic risk scores. J Clin Oncol 2017;35:2240–50.

[14] Shi Z, Yu H, Wu Y, Lin X, Bao Q, Jia H, et al. Systematic evaluation of cancer-specific genetic risk score for 11 types of cancer in the cancer genome atlas and electronic medical records and genomics cohorts. Cancer Med 2019;8:3196–205.

[15] Johnson N, De Ieso P, Migliorini G, Orr N, Broderick P, Catovsky D, et al. Cytochrome P450 allele CYP3A7*1C associates with adverse outcomes in chronic lymphocytic leukemia, breast, and lung cancer. Cancer Res 2016;76:1485–93.

[16] Aminkeng F, Bhavsar AP, Visscher H, Rassekh SR, Li Y, Lee JW, et al. A coding variant in RARG confers susceptibility to anthracycline-induced cardiotoxicity in childhood cancer. Nat Genet 2015;47:1079–84.

[17] Fachal L, Gómez-Caamaño A, Barnett GC, Peleteiro P, Carballo AM, Calvo-Crespo P, et al. A three-stage genome-wide association study identifies a susceptibility locus for late radiotherapy toxicity at 2q24.1. Nat Genet 2014;46:891–4.

[18] McGranahan N, Rosenthal R, Hiley CT, Rowan AJ, Watkins TBK, Wilson GA, et al. Allele-specific HLA loss and immune escape in lung cancer evolution. Cell 2017;171:1259–71 e11.

[19] Chatrath A, Przanowska R, Kiran S, Su Z, Saha S, Wilson B, et al. The pan-cancer landscape of prognostic germline variants in 10,582 patients. Genome Med 2020;12:15.

[20] Jostins L, Ripke S, Weersma RK, Duerr RH, McGovern DP, Hui KY, et al. Host-microbe interactions have shaped the genetic architecture of inflammatory bowel disease. Nature 2012;491:119–24.

[21] Ferreira MAR, Matheson MC, Duffy DL, Marks GB, Hui J, Le Souëf P, et al. Identification of IL6R and chromosome 11q13.5 as risk loci for asthma. Lancet 2011;378:1006–14 (London, England).

[22] Himes BE, Jiang X, Hu R, Wu AC, Lasky-Su JA, Klanderman BJ, et al. Genome-wide association analysis in asthma subjects identifies SPATS2L as a novel bronchodilator response gene. PLoS Genet 2012;8:e1002824.

[23] Raychaudhuri S, Thomson BP, Remmers EF, Eyre S, Hinks A, Guiducci C, et al. Genetic variants at CD28, PRDM1 and CD2/CD58 are associated with rheumatoid arthritis risk. Nat Genet 2009;41:1313–8.

[24] Bønnelykke K, Matheson MC, Pers TH, Granell R, Strachan DP, Alves AC, et al. Meta-analysis of genome-wide association studies identifies ten loci influencing allergic sensitization. Nat Genet 2013;45:902–6.

[25] Han JW, Zheng HF, Cui Y, Sun LD, Ye DQ, Hu Z, et al. Genome-wide association study in a Chinese Han population identifies nine new susceptibility loci for systemic lupus erythematosus. Nat Genet 2009;41:1234–7.

[26] Orlando G, Law PJ, Palin K, Tuupanen S, Gylfe A, Hanninen UA, et al. Variation at 2q35 (PNKD and TMBIM1) influences colorectal cancer risk and identifies a pleiotropic effect with inflammatory bowel disease. Hum Mol Genet 2016;25:2349–59.

[27] Liu TC, Stappenbeck TS. Genetics and pathogenesis of inflammatory bowel disease. Annu Rev Pathol 2016;11:127–48.

[28] Wang C, Mendonsa GR, Symington JW, Zhang Q, Cadwell K, Virgin HW, et al. Atg16L1 deficiency confers protection from uropathogenic Escherichia coli infection in vivo. Proc Natl Acad Sci USA 2012;109:11008–13.

[29] Marchiando AM, Ramanan D, Ding Y, Gomez LE, Hubbard-Lucey VM, Maurer K, et al. A deficiency in the autophagy gene Atg16L1 enhances resistance to enteric bacterial infection. Cell Host Microbe 2013;14:216–24.

[30] Rioux JD, Xavier RJ, Taylor KD, Silverberg MS, Goyette P, Huett A, et al. Genome-wide association study identifies new susceptibility loci for Crohn disease and implicates autophagy in disease pathogenesis. Nat Genet 2007;39:596–604.

[31] Choi AM, Ryter SW, Levine B. Autophagy in human health and disease. N Engl J Med 2013;368:651–62.

[32] Liu T-C, Kern JT, VanDussen KL, Xiong S, Kaiko GE, Wilen CB, et al. Interaction between smoking and ATG16L1T300A triggers Paneth cell defects in Crohn's disease. J Clin Invest 2018;128:5110–22.

[33] Matsuzawa-Ishimoto Y, Shono Y, Gomez LE, Hubbard-Lucey VM, Cammer M, Neil J, et al. Autophagy protein ATG16L1 prevents necroptosis in the intestinal epithelium. J Exp Med 2017;214:3687–705.

[34] Lassen KG, Kuballa P, Conway KL, Patel KK, Becker CE, Peloquin JM, et al. Atg16L1 T300A variant decreases selective autophagy resulting in altered cytokine signaling and decreased antibacterial defense. Proc Natl Acad Sci USA 2014;111:7741–6.

[35] Zhang H, Zheng L, McGovern DPB, Hamill AM, Ichikawa R, Kanazawa Y, et al. Myeloid ATG16L1 facilitates host-bacteria interactions in maintaining intestinal homeostasis. J Immunol 2017;198:2133–46.

[36] VanDussen KL, Liu TC, Li D, Towfic F, Modiano N, Winter R, et al. Genetic variants synthesize to produce paneth cell phenotypes that define subtypes of Crohn's disease. Gastroenterology 2014;146:200–9.

[37] Liu T-C, Naito T, Liu Z, VanDussen KL, Haritunians T, Li D, et al. LRRK2 but not ATG16L1 is associated with Paneth cell defect in Japanese Crohn's disease patients. JCI Insight 2017;2:e91917.

[38] Raju D, Hussey S, Ang M, Terebiznik MR, Sibony M, Galindo-Mata E, et al. Vacuolating cytotoxin and variants in Atg16L1 that disrupt autophagy promote Helicobacter pylori infection in humans. Gastroenterology 2012;142:1160–71.

[39] Ashkenazi A. Targeting the extrinsic apoptotic pathway in cancer: lessons learned and future directions. J Clin Invest 2015;125:487–9.

[40] Olsen S, Jin L, Fields RC, Yan Y, Ilk Nalbantoglu. Tumor budding in intestinal-type gastric adenocarcinoma is associated with nodal metastasis and recurrence. Hum Pathol 2017;68:26–33.

[41] Lauren P. The two histological main types of gastric carcinoma: diffuse and so-called intestinal-type carcinoma. an attempt at a histo-clinical classification. Acta Pathol Microbiol Scand 1965;64:31–49.

[42] Shi C, Berlin J, Branton PA, Fitzgibbons PL, Frankel WL, Hofstetter WL, et al. Protocol for the examination of specimens from patients with carcinoma of the stomach. 2020. https://documents.cap.org/protocols/cp-giupper-stomach-20-4100.pdf (accessed on December 24, 2020).

[43] Hartman DJ, Ahmad F, Ferris RL, Rimm DL, Pantanowitz L. Utility of CD8 score by automated quantitative image analysis in head and neck squamous cell carcinoma. Oral Oncol 2018;86:278–87.

[44] Kim D, Langmead B, Salzberg SL. HISAT: a fast spliced aligner with low memory requirements. Nat Methods 2015;12:357–60.

[45] Patro R, Duggal G, Love MI, Irizarry RA, Kingsford C. Salmon provides fast and bias-aware quantification of transcript expression. Nat Methods 2017;14:417–9.

[46] Hartley SW, Mullikin JC. QoRTs: a comprehensive toolset for quality control and data processing of RNA-Seq experiments. BMC Bioinform 2015;16:224.

[47] DeLuca DS, Levin JZ, Sivachenko A, Fennell T, Nazaire MD, Williams C, et al. RNA-SeQC: RNA-seq metrics for quality control and process optimization. Bioinformatics 2012;28:1530–2.

[48] Anders S, Pyl PT, Huber W. HTSeq—a python framework to work with high-throughput sequencing data. Bioinformatics 2015;31:166–9.

[49] Robinson MD, McCarthy DJ, Smyth GK. edgeR: a bioconductor package for differential expression analysis of digital gene expression data. Bioinformatics 2010;26:139–40.

[50] Cowardin CA, Ahern PP, Kung VL, Hibberd MC, Cheng J, Guruge JL, et al. Mechanisms by which sialylated milk oligosaccharides impact bone biology in a gnotobiotic mouse model of infant undernutrition. Proc Natl Acad Sci USA 2019;116:11988–96.

[51] Cadwell K, Liu JY, Brown SL, Miyoshi H, Loh J, Lennerz JK, et al. A key role for autophagy and the autophagy gene Atg16l1 in mouse and human intestinal Paneth cells. Nature 2008;456:259–63.

[52] Patel KK, Miyoshi H, Beatty WL, Head RD, Malvin NP, Cadwell K, et al. Autophagy proteins control goblet cell function by potentiating reactive oxygen species production. EMBO J 2013;32:3130–44.

[53] Murthy A, Li Y, Peng I, Reichelt M, Katakam AK, Noubade R, et al. A Crohn's disease variant in Atg16l1 enhances its degradation by caspase 3. Nature 2014;506:456–62.

[54] Bass AJ, Thorsson V, Shmulevich I, Reynolds SM, Miller M, Bernard B, et al. Comprehensive molecular characterization of gastric adenocarcinoma. Nature 2014;513:202–9.

[55] Grimm WA, Messer JS, Murphy SF, Nero T, Lodolce JP, Weber CR, et al. The Thr300Ala variant in ATG16L1 is associated with improved survival in human colorectal cancer and enhanced production of type I interferon. Gut 2016;65:456–64.

[56] Cleynen I, Gonzalez JR, Figueroa C, Franke A, McGovern D, Bortlik M, et al. Genetic factors conferring an increased susceptibility to develop Crohn's disease also influence disease phenotype: results from the IBDchip European Project. Gut 2013;62:1556–65.

[57] Varma M, Kadoki M, Lefkovith A, Conway KL, Gao K, Mohanan V, et al. Cell type- and stimulation-dependent transcriptional programs regulated by Atg16L1 and its Crohn's disease risk variant T300A. J Immunol 2020;205:414–24.

[58] Li Q, Zhou X, Huang T, Tang Y, Liu B, Peng P, et al. The Thr300Ala variant of ATG16L1 is associated with decreased risk of brain metastasis in patients with non-small cell lung cancer. Autophagy 2017;13:1053–63.

[59] Burada F, Ciurea ME, Nicoli R, Streata I, Vilcea ID, Rogoveanu I, et al. ATG16L1 T300A polymorphism is correlated with gastric cancer susceptibility. Pathol Oncol Res 2016;22:317–22.

[60] Castano-Rodriguez N, Kaakoush NO, Goh KL, Fock KM, Mitchell HM. Autophagy in helicobacter pylori infection and related gastric cancer. Helicobacter 2015;20:353–69.

[61] Lee JC, Biasci D, Roberts R, Gearry RB, Mansfield JC, Ahmad T, et al. Genome-wide association study identifies distinct genetic contributions to prognosis and susceptibility in Crohn's disease. Nat Genet 2017;49:262–8.

[62] Brant SR, Okou DT, Simpson CL, Cutler DJ, Haritunians T, Bradfield JP, et al. Genome-wide association study identifies African-specific susceptibility loci in African Americans with inflammatory bowel disease. Gastroenterology 2017;152:206–17 e2.

[63] Cleynen I, Boucher G, Jostins L, Schumm LP, Zeissig S, Ahmad T, et al. Inherited determinants of Crohn's disease and ulcerative colitis phenotypes: a genetic association study. Lancet 2016;387:156–67.

[64] Rivas MA, Avila BE, Koskela J, Huang H, Stevens C, Pirinen M, et al. Insights into the genetic epidemiology of Crohn's and rare diseases in the Ashkenazi Jewish population. PLoS Genet 2018;14:e1007329.

[65] Camargo MC, Kim WH, Chiaravalli AM, Kim KM, Corvalan AH, Matsuo K, et al. Improved survival of gastric cancer with tumour Epstein-Barr virus positivity: an international pooled analysis. Gut 2014;63:236–43.

[66] Pietrantonio F, Miceli R, Raimondi A, Kim YW, Kang WK, Langley RE, et al. Individual patient data meta-analysis of the value of microsatellite instability as a biomarker in gastric cancer. J Clin Oncol 2019;37:3392–400.

[67] Chang WH, Lai AG. The pan-cancer mutational landscape of the PPAR pathway reveals universal patterns of dysregulated metabolism and interactions with tumor immunity and hypoxia. Ann NY Acad Sci 2019;1448:65–82.

[68] Chen L, Peng J, Wang Y, Jiang H, Wang W, Dai J, et al. Fenofibrate-induced mitochondrial dysfunction and metabolic reprogramming reversal: the anti-tumor effects in gastric carcinoma cells mediated by the PPAR pathway. Am J Transl Res 2020;12:428–46.